Photos: DOI: 10.2516/ogst/2013138, IFPEN, X.

Dossier

This paper is a part of the hereunder thematic dossier published in OGST Journal, Vol. 69, No. 3, pp. 379-499 and available online here

Cet article fait partie du dossier thématique ci-dessous publié dans la revue OGST, Vol. 69, n°3 pp. 379-499 et téléchargeable ici

DOSSIER Edited by/Sous la direction de : **J.-F. Argillier**

IFP Energies nouvelles International Conference / Les Rencontres Scientifiques d'IFP Energies nouvelles

Colloids 2012 — Colloids and Complex Fluids: Challenges and Opportunities

Colloids 2012 — Colloïdes et fluides complexes : défis et opportunités

Oil & Gas Science and Technology – Rev. IFP Energies nouvelles, Vol. 69 (2014), No. 3, pp. 379-499
Copyright © 2014, IFP Energies nouvelles

Oil & Gas Science and Technology – Rev. IFP Energies nouvelles, Vol. 69 (2014), No. 3, pp. 405-413
Copyright © 2013, IFP Energies nouvelles
DOI: 10.2516/ogst/2013169

IFP Energies nouvelles International Conference
Rencontres Scientifiques d'IFP Energies nouvelles

Colloids 2012 - Colloids and Complex Fluids: Challenges and Opportunities
Colloids 2012 - Colloïdes et fluides complexes : défis et opportunités

Adsorption and Removal of Organic Dye at Quartz Sand-Water Interface

A. Jada* and R. Ait Akbour

IS2M, CNRS-UHA, 15 rue Jean Starcky, 68057 Mulhouse Cedex - France
e-mail: a.jada@uha.fr

* Corresponding author

Résumé — **Adsorption et désorption d'un colorant organique à l'interface sable de quartz-eau** — Nous avons étudié le transport, la sorption et la désorption d'un cation organique (bleu de méthylène (BM)), à travers un milieu poreux constitué de particules de sable de quartz chargées négativement. Nous avons examiné l'influence des paramètres, tels que : la force ionique de la solution aqueuse, la vitesse de circulation, le pH de la phase aqueuse, la température du milieu et la nature des cations divalents métalliques présents en solution, sur le transport et le dépôt du BM à travers le milieu poreux. Les mesures de la rétention du colorant ont été réalisées en utilisant la technique d'injection-échelon.
Les résultats obtenus ont montré une diminution de la quantité de BM adsorbé sur le quartz lorsque le pH de la phase aqueuse diminue de 9,5 à 4. Une baisse de la quantité de BM adsorbé a été également observée lorsque la force ionique ou le débit augmente. Cependant, l'augmentation de la température a conduit à une augmentation de la quantité de BM adsorbée, ce qui laisse supposer que l'adsorption du BM sur la surface de quartz est de nature endothermique. En présence de cations divalents en solution (Ca^{2+}, Cu^{2+}, Zn^{2+} et Ba^{2+}), la quantité retenue du colorant dépend de la nature du cation. L'ensemble de ces résultats, montre que l'adsorption du colorant basique est contrôlée par les interactions électrostatiques entre la surface négative du quartz et le polluant organique cationique.

Abstract — ***Adsorption and Removal of Organic Dye at Quartz Sand-Water Interface*** — *We studied the transport, sorption and desorption of organic cation (Methylene Blue, MB) through a porous medium consisting of quartz sand particles negatively charged. We examined various parameters such as the ionic strength of the aqueous solution, the flow velocity, the pH of the aqueous phase, the temperature of the medium and the nature of the divalent metal cations present in solution, which affect the transport and the deposition of MB through the porous medium. Step-input experiments were carried out to measure the dye retention. The data showed a decrease in the MB adsorbed amount on the quartz, when the pH of the aqueous phase, or the temperature, decreases, or when the flow rate, or the affinity of the divalent cation (Ca^{2+}, Cu^{2+}, Zn^{2+} and Ba^{2+}) toward the quartz surface increases. The increase in ionic strength leads to a small decrease in the MB adsorbed amount. However, the increase in temperature leads to an increase in the retained MB amount, which suggests that the adsorption of MB on the surface of quartz is endothermic in nature. The overall data indicate that, at ambient temperature, electrostatic interaction forces, which occur between the cationic organic pollutant and the negative surface of the quartz substrate, mainly control the adsorption process.*

INTRODUCTION

Chemical synthetic dyes are widely used in many industrial processes for various purposes such as textile dyeing, paper, and plastic, leather tanning. These dyes are also used in food, pharmaceutical or cosmetic [1, 2]. However, most of the solutions used containing these dyes are discarded as effluents. It has been observed that some of these dyes have toxic and carcinogenic effects [3-5] on aquatic life and on human's health. Thus, for reasons related to human health and to protect the environment, the removal of synthetic dyes from aqueous effluents is of great importance.

Various methods of dye removal, such as, coagulation [6], electrochemical deposition [7], adsorption on different adsorbents, chemical decomposition by oxidation, photodegradation and microbiological discoloration, were used. Biological wastewater treatment processes, were found to be ineffective for the removal of dyes [8]. However, the removal of dyes from water by their adsorption on solid supports is one of powerful and low cost treatment processes. In this method, adsorbents such as activated carbon and clays are used. Activated carbon is the most successfully used adsorbent [9-13], but its cost limits its use, especially in developing countries. Therefore, there is a need to find an effective and low cost material as an alternative adsorbent for removing the dyes from water. Among the materials that fulfil these requirements, natural adsorbents such as clays and clay minerals [14-17], zeolites [18], agricultural materials [19-21], cellulosic materials, and various industrial wastes have been investigated in various water depollution studies [22-25]. However, very few studies have focused on the use of quartz sand, as an adsorbent for the removal of dyes from water [26, 27].

The aim of the present work is to study the adsorption of Methylene Blue (MB) from water onto the surface of quartz sand or Fontainebleau sand, which is a cheap and abundant adsorbent. The use of quartz sand as adsorbent will allow us mimic the natural conditions found in hydro systems (soils, aquifers, etc.). In addition, the purpose of this study is to elucidate the mechanism of MB adsorption on the quartz surface, and to investigate the influence on the dye retention of various parameters such as the ionic strength, the flow rate, the pH of the aqueous phase, the temperature, and the nature of the divalent cations present in the aqueous phase.

1 EXPERIMENTAL PART

1.1 Porous Medium

The quartz sand used is a Fontainebleau sand purchased from *Prolabo*. It contains mainly quartz according to the elementary analysis (Si = 45.03%, O = 52.18%, C < 0.3%, H < 0.3%, Ca = 100 ppm, Al = 185 ppm, Mg < 10 ppm, Na < 50 ppm, Fe = 150 ppm). The mean grain diameter, *Dm*, of the sand, is *Dm* = 233.6 ± 46 µm, as determined by Scanning Electron Microscopy (SEM) image analysis (*Fig. 1*), and its isoelectric point IEP = 2.44, as measured by microelectrophoresis (*Fig. 2*).

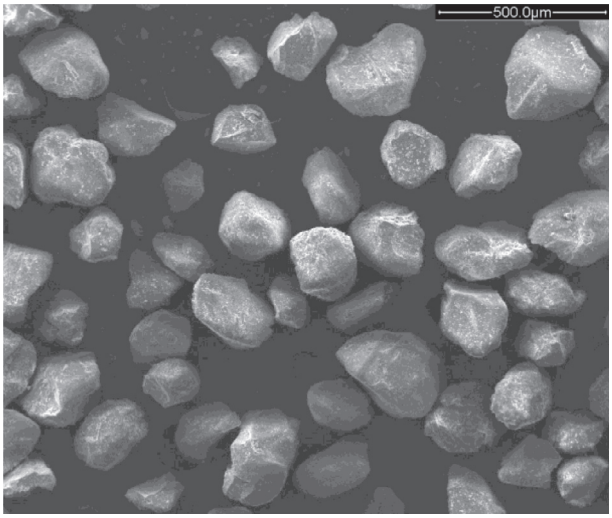

Figure 1

Fontainebleau sand particles as observed by Scanning Electronic Microscopy (MEB).

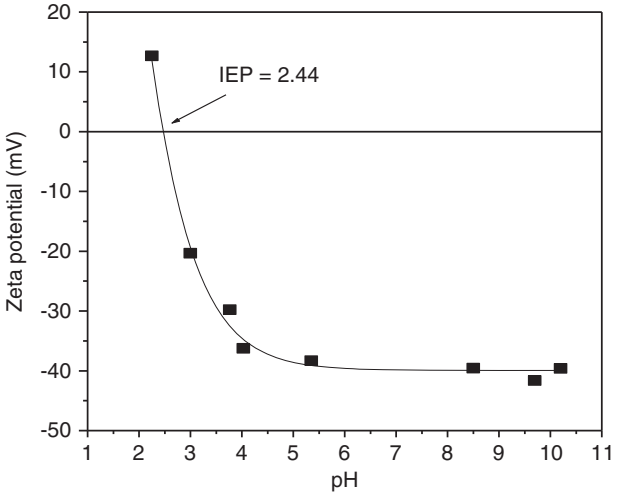

Figure 2

Zeta potential of Fontainebleau sand particles aqueous dispersions. NaCl = 10^{-3}M, 0.2 wt% of the sand in water.

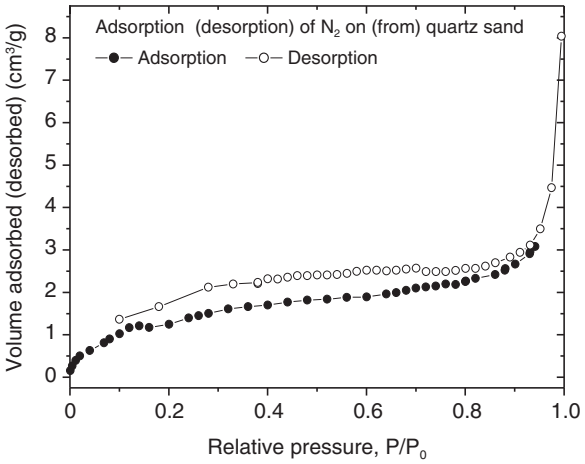

Figure 3

Adsorption-desorption isotherms of nitrogen at 77 K, on Fontainebleau.

In addition, the sand's surface area was measured by using Micromeritics ASAP 2000 surface area analyser. The adsorption-desorption isotherms were obtained by measuring, respectively, the adsorbed and desorbed volumes of N_2 at 77 K and relative pressure P/P_0 ranging from 0 to 1, as depicted in Figure 3. The sample specific surface area is 5.1 ± 0.1 $m^2.g^{-1}$, as determined in the relative pressure range $0.05 < P/P_0 < 0.35$ according to the BET method [28].

It should be noted that in the present work, the quartz sand specific surface area, was also measured in aqueous medium by titration of the negatively charged sand particles by the MB cations. The data gives a specific surface area value of 6.6 ± 0.1 $m^2.g^{-1}$, which is 25% higher than the value found for the quartz sand powder by the BET method.

1.2 Dye (Methylene Blue, MB)

The dye used is Methylene Blue (MB), supplied from Merck. This basic dye belongs to the class of thiazine dyes. Its chemical formula is $C_{16}H_{18}ClN_3S$, and its structural formula is given below (*Fig. 4*). The MB dye is used in various chemical industries, such as textile dyeing, biology, pharmacy, and as an antiseptic. The maximum solubility of MB in water, at 20°C, is equal to 50 $g.L^{-1}$.

1.3 Reagents

All chemical reagents employed in this work are of purity >99.5%, and the aqueous solutions were prepared using, in all instances, bidistilled water. The ionic strength was fixed by using sodium chloride (NaCl) as salt, (except when indicated). The pH values of the samples were varied in the range 4; 6 and 9.5, by adding to the aqueous phase small amounts of sodium hydroxide (NaOH) or hydrochloric acid (HCl) aqueous solutions. Aqueous solutions of calcium chloride ($CaCl_2$), copper chloride ($CuCl_2$), zinc chloride ($ZnCl_2$) and barium chloride ($BaCl_2$), were prepared and used to study the effects of nature of the divalent cations on transport and deposition of MB in a saturated porous medium of quartz sand.

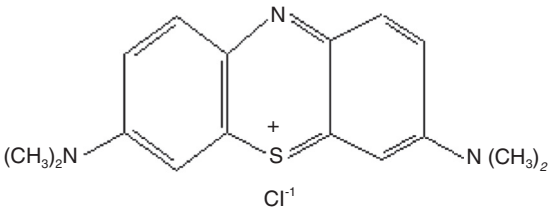

Figure 4

Methylene Blue (MB) structure.

1.4 Experimental Device

The experimental device consisted of three following components:

- a cylindrical column containing the quartz sand made of *Altuglas* and fitted with a jacket thermostated (length, $L = 10$ cm; inner diameter, $D = 1$ cm);
- a syringe pump (Perfusor® secura) to control the flow rate;
- a fraction collector, and a pH-meter allowing the continuous measurement of pH at the column outlet.

The experimental device, held vertically, is fed from bottom to top, in order to facilitate degassing and to reduce the non-uniform flow rise. It should be noted that all the materials used in the experimental device, had demonstrated by preliminary experiments to be non-adsorptive toward MB in the conditions used. Experiments were conducted at room temperature (20 ± 2°C) (except when indicated). In addition, the bottle containing the MB injected solution is made with amber glass to prevent photochemical degradation of the dye molecule, and it was kept under nitrogen atmosphere during all the column experiments.

1.5 Column Experiments

1.5.1 Determination of the Column Pore Volume and Porosity by Using a Tracer

For each experiment, the mass of quartz sand in the column was weighted accurately to be about 9.5 ± 0.2 g.

The column was filled with sand, vacuum packed, and then saturated with degassed bi-distilled water. Washing the column of sand was carried out by continuous injection of bidistilled water, until the obtention of the same inlet and outlet values, of the pH and the conductivity. Both ends of the column were sealed with a device, allowing the immobilization of the quartz sand particles (Glass sintered PTFE), and the obtention of uniform distribution of the liquid flow at the inlet and outlet of the column.

It should be noted that pre-treatment of sand with bi-distilled water, was made in order to avoid the release of fines during the MB flow experiments.

The column outflow for conservative tracer experiments (Potassium Iodide, KI, 20 mg.L^{-1}), was monitored with a UV-visible spectroscopy at λ = 234 nm. Such tracer experiments were made in order to determine the column characteristics such as the pore volume, V_p, and the absolute porosity, ε. The latter is defined as the ratio of the pore volume V_p (cm^3) to the volume of the column V_c (cm^3), and it is given by Equation (1):

$$\varepsilon = V_P/V_C \quad (1)$$

Typical column parameters were V_p = 2.29 mL and ε = 0.42, for 9.5 ± 0.2 g sand mass.

The Peclet number, P_e, was determined using two parameters, the residence time t_s (the time corresponding to the inflection point of the tracer breakthrough curve) and Δt, determined as shown in Figure 5, and using Equation (2) below [29]:

$$P_e = 4\pi(t_s/\Delta t)^2 - 1 \quad (2)$$

1.5.2 Injecting Through the Porous Medium, Aqueous Solutions Containing or not the MB Cations

In a first step, the porous medium is saturated by continuous injection, at constant flow and during one day, of MB free aqueous solution (blank experiments at given pH and ionic strength, *I*), until a steady state is reached. Then, in a second step, MB solution is injected continuously, under the same conditions as those made for the blank tests into the column, until equilibrium. In a third step, elution of sorbed MB is performed with MB free aqueous phase having the same values of pH and ionic strength, than those previously used in injecting the dye into the porous medium.

1.5.3 Column Outlet Fractions Analysis

The fractions at the outlet of the column were collected at constant volume, and their fluorescence excitation spectra were measured by using a spectrofluorimeter (*Shimadzu* RF-5001). The fluorescence excitation spectra

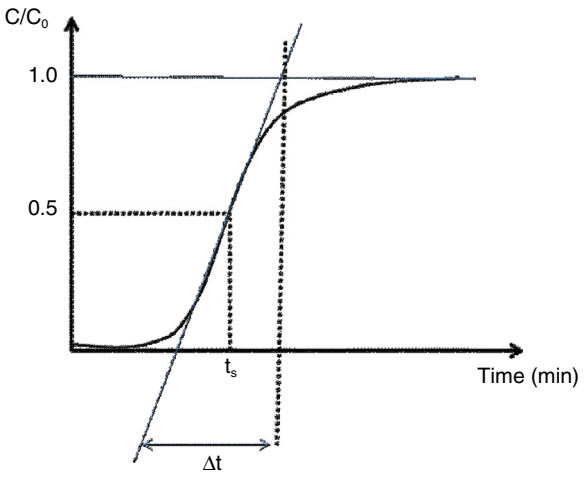

Figure 5

Tracer (KI) breakthrough curve.

were recorded at the excitation wavelength range 450-720 nm and emission wavelength = 750 nm. From the integrated fluorescence intensities of, the outlet or effluent fractions, and the known MB aqueous solutions series (recorded under identical conditions), the MB residual concentrations in the collected fractions, *C*, were then determined.

In the following, only the breakthrough curves dealing with the effect of the ionic strength, *I*, will be presented. These curves will be expressed as C/C_0 *versus* V/V_p. The ratio (C/C_0) is the normalized effluent concentration and the (V/V_P) is normalized injected solution volume; *C* is the total MB concentration measured in each effluent fraction, *V* is the cumulated volume eluted since the beginning of the MB injection, V_p the pore volume, and C_0 the inlet MB concentration. From the breakthrough curves dealing, with the effects of various parameters (flow rate, pH, temperature and the nature of divalent cation), we determined the amounts of MB adsorbed, M_{ads}, and the MB desorbed, M_{des}, at the quartz sand-aqueous solution interface. Note that in all the experiments, each breakthrough curve is composed of two fronts: an adsorption front followed by a desorption one.

2 RESULTS AND DISCUSSIONS

2.1 Effect of the Ionic Strength

Figure 6 shows the adsorption fronts of the breakthrough curves dealing with the effect of the ionic

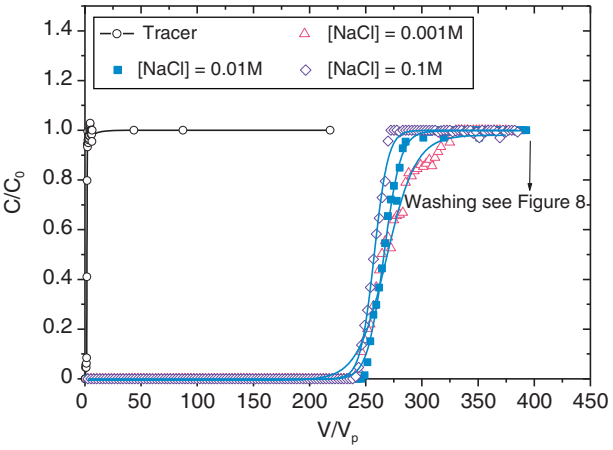

Figure 6

Effect of the ionic strength, I as fixed by NaCl, on MB adsorption from water onto quartz sand. Initial MB concentration, C_0 = 1 ppm; pH = 6, flow velocity, Q = 60 mL.h^{-1}, temperature T = 20°C.

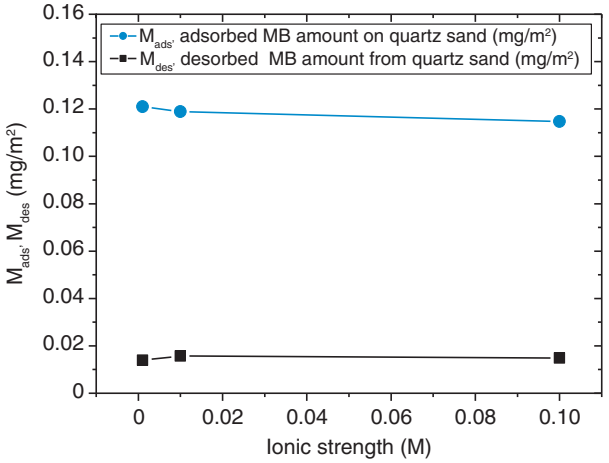

Figure 7

Effect of the ionic strength, I as fixed by NaCl, on adsorbed (M_{ads}) and desorbed (M_{des}), MB amounts at quartz sand-water interface. Initial MB concentration, C_0 = 1 ppm; pH = 6, flow velocity, Q = 60 mL.h^{-1}, temperature T = 20 °C.

strength, I. This figure indicates clearly the influence of ionic strength on the transport and adsorption of MB through the quartz sand column.

As can be seen in Figure 6, they are small differences between the adsorption fronts obtained at various values of the ionic strength. Moreover, masses balances were calculated as the difference between the breakthrough data of the conservative tracer and MB for each experiment, and for both adsorption and desorption fronts. The variation of the MB amounts sorbed, M_{ads}, and released, M_{des}, *versus* the ionic strength, I, are presented in Figure 7, which shows that M_{ads} decreases slightly when the ionic strength, I, of the solution increases.

The sorption of MB on the quartz grains in the presence of NaCl salt can be explained by competition between the MB and Na^+ cations, towards the negative sites of the quartz surface (pH > IEP), and the zeta potential magnitude, which decreases, as the concentrations of various ionic species, increase at the quartz sand-solution interface. The MB adsorption on the quartz surface results from the ionic nature of the interaction occurring between the MB cations and the sand negative surface sites [30].

A decrease in the magnitude of zeta potential at the quartz – solution interface, by increasing the ionic strength of the medium, will be in favour of a decrease in the coulombic attraction between the quartz negative surface sites and the MB cations, which explains the decrease of the MB adsorbed amount on the solid surface. This behaviour in the presence of salt, of cationic dye through negatively porous medium, is in agreement

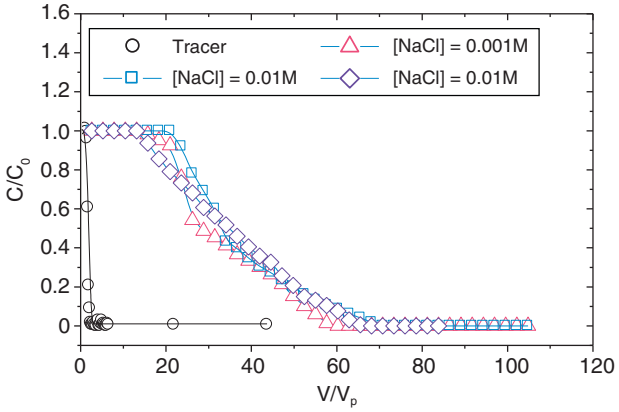

Figure 8

Effect of the ionic strength, I as fixed by NaCl, on MB desorption from quartz sand. Initial MB concentration, C_0 = 1 ppm; pH = 6, flow velocity, Q = 60 mL.h^{-1}, temperature T = 20°C.

with the works reported by other authors [31-35]. More recently, Bilgiç [36], found that the adsorption capacities of MB dye on bentonite and sepiolite decrease with increasing ionic strength.

The elution curves as depicted in Figure 8, show at the beginning the presence of plateaus which are followed, at V/Vp > 20, by diffuse fronts of desorption.

The MB released amount, M_{des}, as calculated from the mass balance, is much lower than the MB adsorbed amount, M_{ads}, as can be seen in Figure 7. The M_{des}

values represent about 8% of M_{ads} values. This behaviour is characteristic of an irreversible adsorption or pseudo-irreversible process, and may due to the strong adsorption, by attractive electrostatic forces, of MB cations on the quartz sand surface.

In the following, only the variations with the various parameters (flow rate, pH, temperature and the nature of divalent cation), of the MB adsorbed and released amounts, M_{ads} and M_{des}, at the quartz sand-aqueous solution interface, will be presented.

2.2 Effect of the Flow Rate

In this experiment series, we studied the influence of the flow rate on the mobility of MB (C_0 = 1 ppm) through the porous medium, in the presence of 10^{-3} M NaCl. The MB adsorbed and released amounts, M_{ads} and M_{des}, at the quartz sand-aqueous solution interface, and at different flow rates, are shown in Figure 9. As can be observed in the figure, M_{ads} and M_{des}, increase both when the flow rate, Q, decreases from Q = 90 mL.h^{-1} to Q = 45 mL.h^{-1}.

These variations may be due to the decrease, at high flow rate, of the diffusion and the penetration of the MB solute, to the quartz sand surface.

Qualitatively, the Peclet number, P_e, which is a relevant parameter in the study of transport phenomena in fluid flows, represents the ratio of two time characteristics, that of transfer by convection and that of transfer by diffusion. The Peclet number, P_e, encompasses in a dimensionless form, the impact of both the flow rate and the particle size, on the MB adsorbed mass on the quartz sand surface [37]. Moreover, it was shown that the collection efficiency, η, defined for a spherical collector, as the ratio between, the flow of particles retained by the collector and the incident flux, is related to P_e by a power law having an exponent of $-2/3$ or -1, depending on whether the deposit is limited, respectively, by diffusion (DLD) or by reaction (RLD) [37]. Thus, according to these power laws, the fraction of MB retained on the quartz surface decreases when the flow rate, Q, increases. Our experimental data are in a good agreement with the theoretical predictions using the colloidal approach.

Our results agree also with the data reported by Lin *et al.* [38]. According to these authors, the increase in the flow rate, Q, disadvantages the acidic dye adsorption on montmorillonite. Our findings are consistent with the work reported by Benkli *et al.* [18], showing that the adsorption of hexadecyl trimethyl ammonium bromide on zeolites, depends on the flow rate. The effect of flow rate on the retention of MB, results from the duration time when the fluid is in contact with the quartz surface (contact time). Thus, when the flow rate is low, the number of adsorbed MB cations on the solid surface is higher, as resulting from the long contact time occurring between the fluid molecules and the quartz surface.

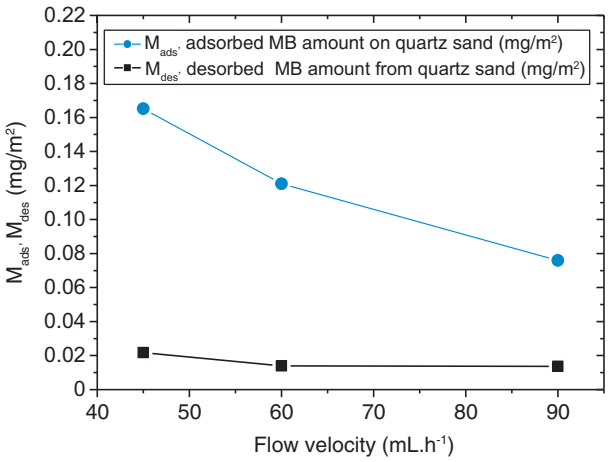

Figure 9

Effect of flow velocity, Q, on adsorbed (M_{ads}) and desorbed (M_{des}), MB amounts at quartz sand-water interface. Initial MB concentration, C_0 = 1 ppm, ionic strength, I = 10^{-3}M (NaCl), pH = 6, temperature T = 20°C.

2.3 Effect of the Aqueous Phase pH

We carried out adsorption experiments of MB on the quartz sand surface, at three values of the aqueous phase pH: pH = 4, 6 and 9.5.

The observed increases of M_{ads} and M_{des} with the increase of the aqueous phase pH, as shown in Figure 10, indicate that the pH is a parameter that strongly affects the adsorbed MB amount. The influence of the aqueous phase pH on the variation of the MB sorbed amount, results in the bonding forces involved in the formation of the MB-silica complex. Such bonding interactions include electrostatic, as well as Van der Waals forces [39]. Kar *et al.*, [40], have reported similar pH effect, on the adsorption of dye molecules, at mineral-water interface. According to these authors, the dye adsorption capacity on silicates increases with increasing the pH of the aqueous phase. Moreover, recently, Tsai *et al.* [41], found that the adsorption of basic dye from aqueous solution onto clay surface, reached its maximum value in basic medium (*i.e.*, at pH = 10).

2.4 Effect of Temperature

The influence of the temperature on the transport of the MB basic dye through the porous medium is shown in

Figure 11, which indicates that the increase of temperature promotes the MB retention. Such dye behaviour proves that the adsorption of MB at the quartz sand-aqueous solution interface is an endothermic process. The same thermal behaviour was observed by Ghosh and Bhattacharyya [16], when they studied the adsorption of MB on kaolinite. Further, Dogan and Alkan [15], examined the retention of methyl violet onto perlite, and they found that the rate of methyl violet adsorption increased with increasing temperature and pH of the aqueous phase. From the breakthrough data and mass balances calculations, the increase in temperature from 293 K to 333 K, leads to an increase in M_{ads} from 0.12 to 0.17 mg/m^2, *i.e.* an increase of about 42%. However, the same increase in temperature does not show significant change of M_{des}, as can be seen in Figure 11. Increasing the temperature leads to an increase of thermal agitation, and also to an increase of the diffusion rate of the ions, resulting in an enhancement of the exchange, and/or displacement, of Na^+ ions, immobilized near the surface solid, by MB cations. Finally, the adsorption of MB on the quartz sand particles involves two main steps: a first transport step, during which the MB molecules diffuse from the aqueous phase to the quartz surface, and a second step (anchoring or binding step) in which the MB molecules adsorb on the solid surface. The kinetics of transport and binding of MB molecules at solid-liquid interface, are controlled by different factors, such as ionic strength, pH of the aqueous phase, and the temperature of the medium.

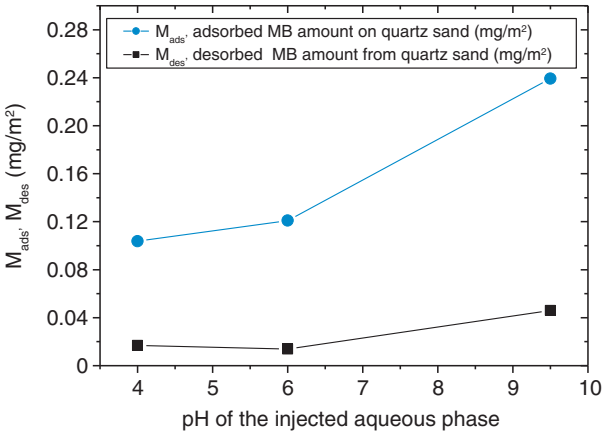

Figure 10

Effect of the aqueous phase pH, on adsorbed (M_{ads}) and desorbed (M_{des}), MB amounts, at quartz sand-water interface. Initial MB concentration, C_0 = 1 ppm, ionic strength, I = 10^{-3}.

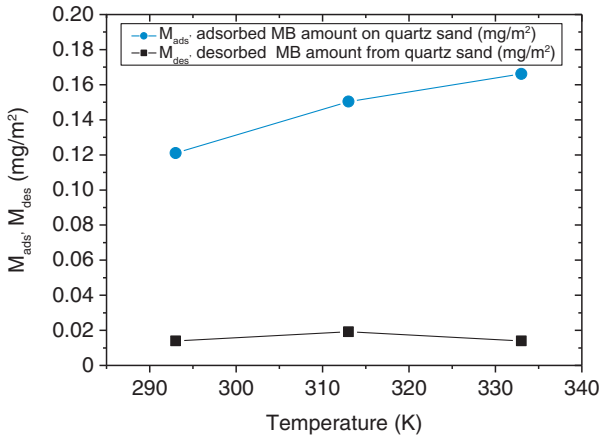

Figure 11

Effect of temperature, T, on adsorbed (M_{ads}) and desorbed (M_{des}), MB amounts at quartz sand-water interface. Initial MB concentration, C_0 = 1 ppm, ionic strength, I = 10^{-3}M.

2.5 Effect of the Divalent Cation Nature

In this experiment series, we examined the effect of divalent metal ions on the MB adsorption from water onto quartz sand. The divalent cations used, were in the form of metal chloride salts ($CaCl_2$, $CuCl_2$, $ZnCl_2$ and $BaCl_2$), at a concentration of 10^{-3}M.

The M_{ads} and M_{des} were calculated from the mass balances of the breakthrough data, and their variations with the divalent cation nature, are presented in Figure 12. The

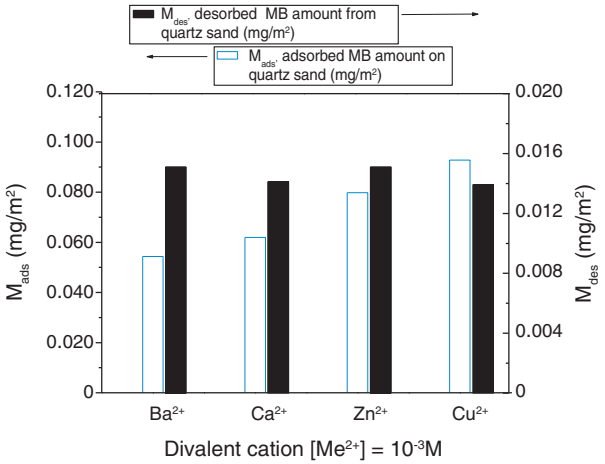

Figure 12

Effect of the divalent cation Me^{2+}, on adsorbed (M_{ads}) and desorbed (M_{des}), MB amounts at quartz sand-water interface. Initial MB concentration, C_0 = 1 ppm, [Me^{2+}] = 10^{-3}M (Me^{2+} = Ca^{2+}, Cu^{2+}, Zn^{2+} and Ba^{2+}), pH = 6, temperature T = 20°C.

results show that the MB adsorbed mass, M_{ads}, decreases in the sequence: $Cu^{2+} > Zn^{2+} > Ca^{2+} > Ba^{2+}$. This behaviour may be explained by the cation affinity toward the solid support. Thus, the saturation of the quartz sand by the divalent cations ($Me^{2+} = Ca^{2+}$, Cu^{2+}, Zn^{2+} and Ba^{2+}) reduce the number of the solid negative sites, resulting in reduction of the electrostatic attraction between the MB cations and the solid surface. However, the decrease in the electrostatic attraction between the MB cations, and the solid surface depends on the ionic radius, r_i, of the divalent cation, Me^{2+}, present in the aqueous solution. Thus, according to Coulomb's law, the divalent cation, Me^{2+}, having the largest ionic radius, r_i, (non-hydrated radius), is preferentially adsorbed on the solid surface [42]. The ionic radii of different divalent cations Me^{2+}, decrease in the following sequence:

$$Ba^{2+}(r_i = 140\ \text{pm}) > Ca^{2+}(r_i = 100\,\text{pm}) > Zn^{2+}(r_i = 74\,\text{pm}) > Cu^{2+}(r_i = 73\,\text{pm})$$

Therefore, the strong adsorptions of MB cations on the quartz sand, as observed in the presence of Cu^{2+} and Zn^{2+} ions, result from the slight reduction of the quartz negative surface charge and/or the low affinities of the metal cations toward the solid. On the other hand, the low adsorptions of MB cations on quartz particles, in the presence of Ca^{2+} and Ba^{2+} ions, are due to the strong reduction of the quartz negative surface charge and/or to the higher affinities of the metal cations toward the solid.

In summary, the adsorption of MB cations on the quartz surface, in the presence of divalent metal cation Me^{2+}, depends on both, the metal cation affinity toward the solid surface, and its hydration by water molecules. Metal cation having smaller ionic radius, r_i, is more hydrated than cation with higher r_i, resulting in higher mobility towards the solid surface of the smaller metal cation. Increasing the metal cation Me^{2+} ionic radius leads, to decrease of its hydration shell thickness, and to an increase of its affinity toward the solid surface, resulting hence in a decrease of the MB adsorbed amount on the solid surface.

CONCLUSION

A natural quartz sand column was used to study the transport, retention, and release of Methylene Blue (MB). The quartz sand was selected as adsorbent, due to its availability and low cost. The data presented in this work show the effects of various parameters, such as ionic strength, flow rate, pH of the aqueous phase, the temperature of the medium, and the nature of the divalent cation, on the transport and the retention of MB dye, through the porous medium. The main results are summarized as follows:

- the retained MB amount, in the quartz sand porous medium, decreases significantly when the flow rate increases. However, a slight decrease in the retained MB amount occurs when the ionic strength of the aqueous phase increases;
- the fraction of MB deposited on the quartz increases by increasing either the temperature of the medium, or by raising the pH of the aqueous phase;
- the presence of metal divalent cations in the medium decreases in all instances, the adsorbed MB amount. However, such decrease depends on both, the metal cation affinity toward the solid surface, and its hydration by water molecules;
- the adsorption of MB on the quartz sand particles is endothermic nature and it is irreversible.

The overall data provide useful information to elucidate the mechanisms of complex formation, occurring in soil and groundwater, between inorganic or organic cations and the quartz sand surface.

REFERENCES

1 Crini G. (2006) Non-conventional low-cost adsorbents for dye removal: A review, *Bioresour. Technol.* **97**, 1061-1085.

2 Wu F.C., Tseng R.L. (2008) High adsorption capacity NaOH-activated carbon for dye removal from aqueous solution, *J. Hazard Mater.* **152**, 1256-1267.

3 McKay G., Otterburn M.S., Aga D.A. (1985) Fullers earth and Fired clay as adsorbent for dye stuff, equilibrium and rate constants, *Water Air Soil Pollut.* **24**, 307-322.

4 Gregory A.R., Elliot S., Khuge P. (1991) Ames testing of direct black 3B parallel carcinogenecity, *J. Appl. Toxicol.* **1**, 308-313.

5 Liakou S., Pavlou S., Lyberatos G. (1997) Ozonation of azo dyes, *Water Sci. Technol.* **35**, 279-286.

6 Solozhenko E.G., Soboleva N.M., Goncharuk V.V. (1995) Decolourization of azodye solutions by Fenton's oxidation, *Water Res.* **29**, 2206-2210.

7 Lin S.H., Peng C.F. (1994) Treatment of textile wastewater by electrochemical method, *Water Res.* **28**, 277-282.

8 Walker G.M., Weatherley L.R. (1997) Adsorption of acid dyes onto granular activated carbon in fixed beds, *Water Res.* **31**, 2099-2101.

9 Yang X.Y., Al-Duri B. (2001) Application of branched pore diffusion model in the adsorption of reactive dyes on activated carbon, *Chem. Eng. J.* **83**, 15-23.

10 Karaca S., Gürses A., Açikyildiz M., Ejder M. (2008) Adsorption of cationic dye from aqueous solutions by activated carbon, *Microporous Mesoporous Materials* **115**, 376-382.

11 Kannan N., Sundaram M.M. (2001) Kinetics and mechanism of removal of methylene blue by adsorption on various carbons – a comparative study, *J. Dyes Pig.* **51**, 25-40.

12 Walker G.M., Weatherley L.R. (1998) Fixed bed adsorption of acid dyes onto activated carbon, *Environ Pollution* **99**, 133-136.

13 Jia-Ming C., Chia-Yuan W. (2001) Desorption of dye from activated carbon beds: effects of temperature, pH, and alcohol, *Water Res.* **35**, 4159-4165.

14 Ho Y.S., Chiang C.C. (2001) Sorption studies of acid dye by mixed sorbents, *Adsorption-Journal International Adsorption Society* **7**, 139-147.

15 Dogan M., Alkan M. (2003) Adsorption kinetics of methyl violet onto perlite, *Chemosphere* **50**, 517-528.

16 Ghosh D., Bhattacharyya K.G. (2002) Adsorption of methylene blue on kaolinite, *Appl. Clay. Sci.* **20**, 295-300.

17 Rytwo G., Tropp D., Serban C. (2002) Adsorption of diquat, paraquat and methyl green on sepiolite: experimental results and model calculations, *Appl. Clay Sci.* **20**, 273-282.

18 Benkli Y.E., Can M.F., Turan M., Celik M.S. (2005) Modification of organo-Zeolite surface for the removal of reactive azo dyes in fixed-bed reactors, *Water Research* **39**, 487-493.

19 McKay G., El Geundi M., Nassar M.M. (1988) External mass transport processes during the adsorption of dyes onto bagasse pith, *Water Res.* **22**, 1527-1533.

20 Robinson T., Chandran B., Nigam P. (2002) Removal of dyes from an artificial textile dye effluent by two agricultural waste residues, corncob and barley husk, *Environ. Int.* **28**, 29-33.

21 Annadurai G., Juang R.S., Lee D.J. (2002) Use of cellulose-based wastes for adsorption of dyes from aqueous solutions, *J. Hazard. Mater. B* **92**, 263-274.

22 Wang C.C., Juang L.C., Hsu T.C., Lee C.K., Lee J.F., Huang F.C. (2004) Adsorption of Basic Dyes onto Montmorillonite, *J. Colloid Interface Sci.* **273**, 80-86.

23 Jain A.K., Gupta V.K., Bhatnagar A., Suhas (2003) Utilization of industrial waste products as adsorbents for the removal of dyes, *J. Hazard. Mater.* **101**, 31-42.

24 Moussavi G., Khosravi R. (2011) The removal of cationic dyes from aqueous solutions by adsorption onto pistachio hull waste, *Chemical Engineering Research Design* **89**, 2182-2189.

25 Gong R.M., Li M., Yang C., Sun Y.Z., Chen J. (2005) Removal of cationic dyes from aqueous solution by adsorption on peanut hull, *J. Hazard Mater. B* **121**, 247-250.

26 Espantaleón A.G., Nieto J.A., Fernández M., Marsal A. (2003) Use of activated clays in the removal of dyes, *Appl. Clay Sci.* **24**, 105-110.

27 Al-Asheh S., Banat F., Abu-Aitah L. (2003) The removal of methylene blue dye from aqueous solutions using activated and non-activated bentonites, *Adsorpt. Sci. Technol.* **21**, 451-462.

28 Brunauer S., Emmett P.H., Teller E. (1938) Adsorption of gases in multimotecular layers, *J. Am. Chem. Soc.* **60**, 309-310.

29 Schweich D., Sardin M. (1981) Adsorption, partition, ion exchange and chemical reaction in batch reactors or in columns – a review, *J. Hydrology* **50**, 1-33.

30 Jada A., Ait Akbour R., Douch J. (2006) Surface charge and adsorption from water onto quartz sand of humic acid, *Chemosphere* **64**, 1287-1295.

31 Elimelech M., Gregory Y., Jia X., Williams R. (1995) *Particle deposition and aggregation: Measurement, modeling and simulation*, Butterworth-Heinemann, Oxford.

32 Bueno M. (1999) Étude dynamique des processus de sorption–désorption du tributylétain sur un milieu poreux d'origine naturelle, *Thèse de Doctorat*, Université de Pau et des Pays de l'Adour.

33 Johnson P.R., Sun N., Elimelech M. (1996) Colloid Transport in Geochemically Heterogeneous Porous Media: Modeling and Measurements, *Environ. Sci. Technol.* **30**, 3284-3293.

34 Rytwo G., Nir S., Margulies L. (1996) A Model for Adsorption of Divalent Organic Cations to Montmorillonite, *J. Colloid Interface Sci.* **189**, 551-560.

35 Mishael Y.G., Rytwo G., Nir S., Grespin M., Annabi-Bergaya F., van Damme H. (1999) Interactions oh monovalent organic cations with pillared clays, *J. Colloid Interface Sci.* **209**, 123-128.

36 Bilgiç C. (2005) Investigation of the factors affecting organic cation adsorption on some silicate minerals, *J. Colloid Interface Sci.* **281**, 33-38.

37 Rousseau D., Hadi L., Nabzar L. (2008) Injectivity Decline From Produced-Water Reinjection: New Insights on In-Depth Particle-Deposition Mechanisms, *SPEPO* **23**, (4), 525-531.

38 Lin S.H., Juang R.S., Wang Y.H. (2004) Adsorption of acid dye from water onto pristine and acid-actived clays in fixed beds, *J. Hazardous Materials B* **113**, 195-200.

39 Kaouna F., Gaid A., Ait Amar H. (1987) Cinétique d'adsorption du bleu méthylène sur différents types d'argiles kaolinitiques, *Bull. Soc. Chim. Fr* **4**, 581-587.

40 Kar H.S., Mundhara G.L., Sharma G.L., Tiwari J.S. (1991) Sorption-desorption studies of cationic dyes on silica gel pretreated with alkalis in relation to chromatography, *Colloids Surf.* **55**, 23-40.

41 Tsai W.T., Chang Y.M., Lai C.W., Lo C.C. (2005) Adsorption of basic dyes in aqueous solution by clay adsorbent from regenerated bleaching earth, *Applied Clay Science* **29**, 149-154.

42 Alloway B.J. (1995) *Heavy metals in soils*, Alloway B.J. (ed.), (Dir), London Blackie Academic and Professional.

Manuscript accepted in July 2013
Published online in November 2013

Copyright © 2013 IFP Energies nouvelles

Permission to make digital or hard copies of part or all of this work for personal or classroom use is granted without fee provided that copies are not made or distributed for profit or commercial advantage and that copies bear this notice and the full citation on the first page. Copyrights for components of this work owned by others than IFP Energies nouvelles must be honored. Abstracting with credit is permitted. To copy otherwise, to republish, to post on servers, or to redistribute to lists, requires prior specific permission and/or a fee: Request permission from Information Mission, IFP Energies nouvelles, fax. +33 1 47 52 70 96, or revueogst@ifpen.fr.